ADVANCED BIOSYSTEMS

Supporting Information

for *Adv. Biosys.,* DOI: 10.1002/adbi.201900291

In Vitro Platform for Studying Human Insulin Release Dynamics of Single Pancreatic Islet Microtissues at High Resolution

Patrick M. Misun, Burçak Yesildag,* Felix Forschler, Aparna Neelakandhan, Nassim Rousset, Adelinn Biernath, Andreas Hierlemann, and Olivier Frey*

Supporting Information

In-vitro platform for studying human insulin release dynamics of single pancreatic islet microtissues at high resolution

Patrick M. Misun[*]*, Burçak Yesildag*[*]*, Felix Forschler, Aparna Neelakandhan, Nassim Rousset, Adelinn Biernath, Andreas Hierlemann, Olivier Frey*

Numerical Simulation Parameters

The numerical simulations in this article have been conducted using COMSOL Multiphysics®. We include herein the details of the model.

Model Geometry: A 3D model of the liquid phase of the chip including the inlet, outlet, and hanging drop was drawn (see Figure 2b for a 2D cross-section). The PDMS was also included to account for its absorption of Rhodamine 6G.

Model Physics: The transport of Rhodamine 6G or insulin is achieved via convection and diffusion.

The "Laminar Flow" physics interface was used to model flow velocity and pressure in the liquid phase with the following boundary conditions:

- Inlet: 15 µL/min laminar inflow;
- Outlet: null pressure;
- Liquid-PDMS interfaces: no-slip;
- Air-Liquid interface:
    - Slip boundary condition to model the hanging-drop design;
    - No slip boundary condition to model a closed-chip design.

The "Transport of Diluted Species" physics interface was used to model Rhodamine 6G and insulin transport. It includes both diffusive and convective transport in the liquid phase and diffusion into PDMS with a partition coefficient. The diffusion and partition coefficients were taken from the literature. The model was solved with the following boundary conditions:

- Inlet: Target species concentration inflow
    - Rhodamine 6G: step increase then decrease after 10 minutes;
    - Insulin: null concentration;
- Outlet: passive species outflow;
- Liquid-PDMS interfaces (for Rhodamine 6G): Water/PDMS partition coefficient;
- Liquid-microtissue interface (for insulin): Sharp insulin influx from a spherical microtissue into the medium, where the total generated insulin is equal to experimental values and is generated in under one second.

Model Mesh: We used the physics-controlled fine mesh for the “Laminar Flow” model. For the “Transport of Diluted Species” model, the physics-controlled extremely fine mesh was refined at liquid-PDMS interfaces to account for large Rhodamine 6G gradients in the PDMS at the interface.

Model Solver: We solved the steady-state solution of the flow in the hanging drop with the built-in solver. We used this steady-state solution for the convective transport in solving the time-dependent study of the transport of Rhodamine 6G and insulin.

Model Results: We used COMSOL Multiphysics® to draw 2D figures from cut plane data sets and we extracted average values over surfaces and volumes of interest. Figure 2b features a cut plane through the symmetry axis with the flow speed on a logarithmic scale. Figure S1b features the shear stress on the spheroid taken as the viscosity multiplied by the shear rate (calculated in COMSOL). Figure 2c features the average Rhodamine 6G concentration in the same region of interest as the experimental data for the “Average in drop” data set and the average Rhodamine 6G concentration on a spherical microtissue, located at the bottom of the drop, for the “Average on islet” data set. Figure 2d features the prescribed islet secretion rate at the spherical microtissues surface, and the average insulin concentration at the outlet for slip and no-slip boundary conditions at the air-liquid interface. Taking the average of the latter values over the sampling period results in modelling the expected measured concentration. This demonstrates the sampling aliasing that is caused by the no-slip boundary condition. Movie S3 features a cut plane through the symmetry axis that shows how this aliasing occurs.

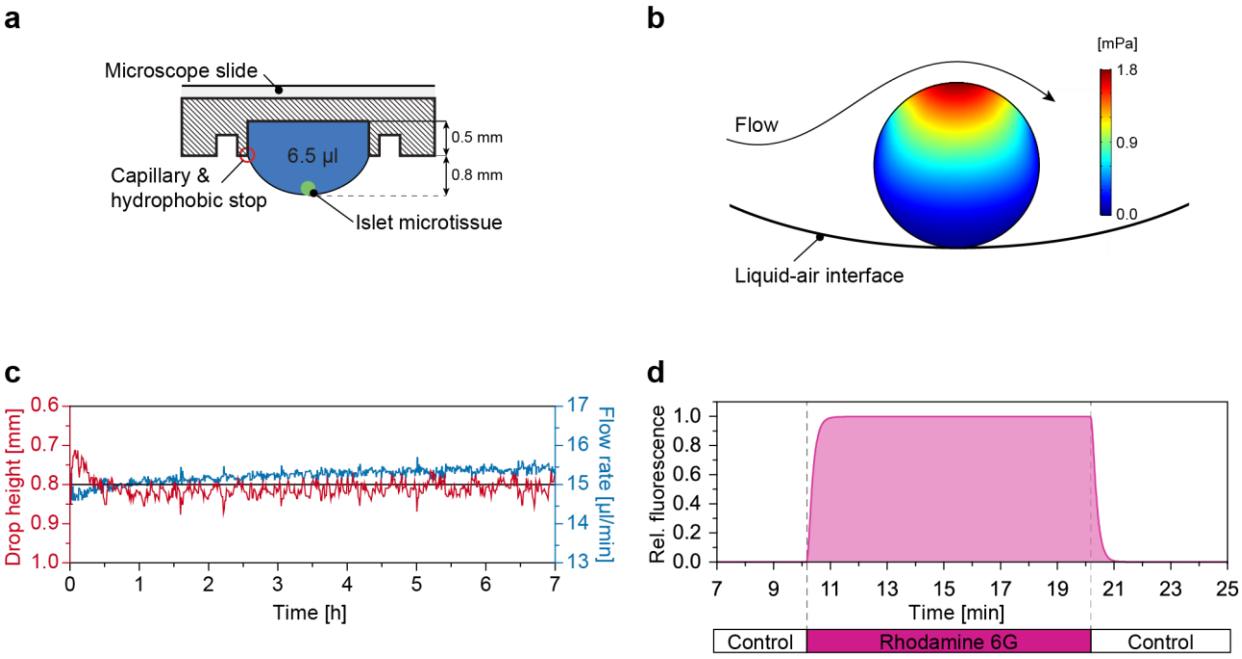

Figure S1: a) Cross-section through a microfluidic hanging drop chip hosting an islet microtissue. The islet is located at the liquid-air interface at the bottom of the hanging drop and is fully accessible. **b**) Modeling results of shear-stress on the islet microtissue (150 µm diameter) in a hanging drop (0.8 mm in height), caused by medium perifusion at 15 µl min^{-1}. **c**) Stable operation of the perfused hanging drop. The height of the hanging drop was kept stable at 780 ± 12 µm, while it was perfused at a constant flow rate of 15 µl min^{-1}. **d**) A fluorescent dye (Rhodamine 6G) was infused into the chip, and the fluorescence in the drop was measured every 7 seconds. A full medium exchange in the hanging drop was reached after ~2 min.

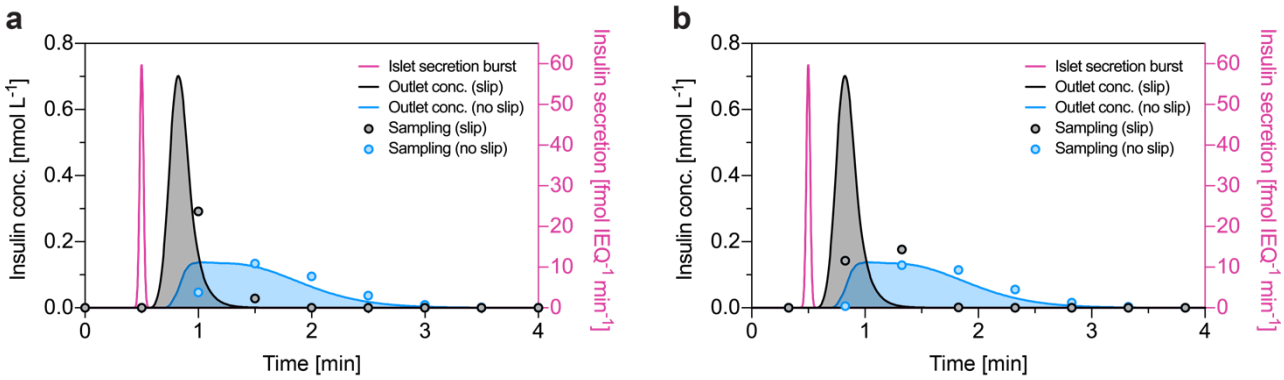

Figure S2: Modeling results of insulin concentration at the outlet of the chip following a sharp 1-s-long insulin secretion burst at the islet (purple), which is equivalent to an experimentally measured secretion of 2.5 fmol over one sample interval. The resulting outlet concentration were obtained assuming either slip (black) or no-slip (blue) boundary conditions at the bottom of the drop. The resulting expected experimental sample points are shown for a sampling rate of two samples per minute for both, slip (black dots) and no-slip (blue dots) boundary conditions. **a**) In-phase sampling. A secretion peak was resolved with one sampling point (black dots). **b**) Out-of-phase sampling. A secretion peak was resolved with two sampling points (red dots).

Movie S3: a) Insulin secretion from an islet microtissue and the flow-mediated transport of secreted insulin at the liquid-air surface for slip (black) and no-slip (blue) conditions. A sharp 1-s-long secretion burst of 2.5 fmol insulin of the islet was simulated. **b**) Modeling of insulin concentration at the outlet of the chip. The resulting concentration at the outlet was obtained assuming either slip- (black) or no-slip (blue) boundary conditions at the bottom of the drop for in-phase sampling. **c**) The resulting sample points and concentrations are shown for a sampling rate of two samples per minute for both, slip- (black dots) and no-slip (blue dots) boundary conditions.

Table S4: Applying a flow-based glucose-stimulated insulin secretion protocol in the presented microfluidic hanging-drop perifusion system can be used to extract detailed characteristics of insulin release.

Glucose concentration	GSIS Phases	Characteristics of insulin release dynamics
2.8 mM	**Baseline**	Average secretion rate
		Total secreted insulin
		Variability of secretion rate
	Pre-stimulation	Response time
		Average secretion rate
		Total secreted insulin
		Variability of secretion rate
16.7 mM	**Dip**	Appearance of dip
		Dip (minimal) secretion
	1st Phase	Response time
		Average secretion rate
		Total secreted insulin
		Time to reach peak
		Peak (maximum) secretion
	2nd Phase	Average secretion rate
		Total secreted insulin
		Appearance of oscillations
		Frequency of oscillations
		Insulin depletion (relaxation in insulin release)
		Relaxation time after switching to low glucose
2.8 mM	**Post-stimulation**	Response time (Relaxation)
		Average secretion rate
		Total secreted insulin
		Variability of secretion rate

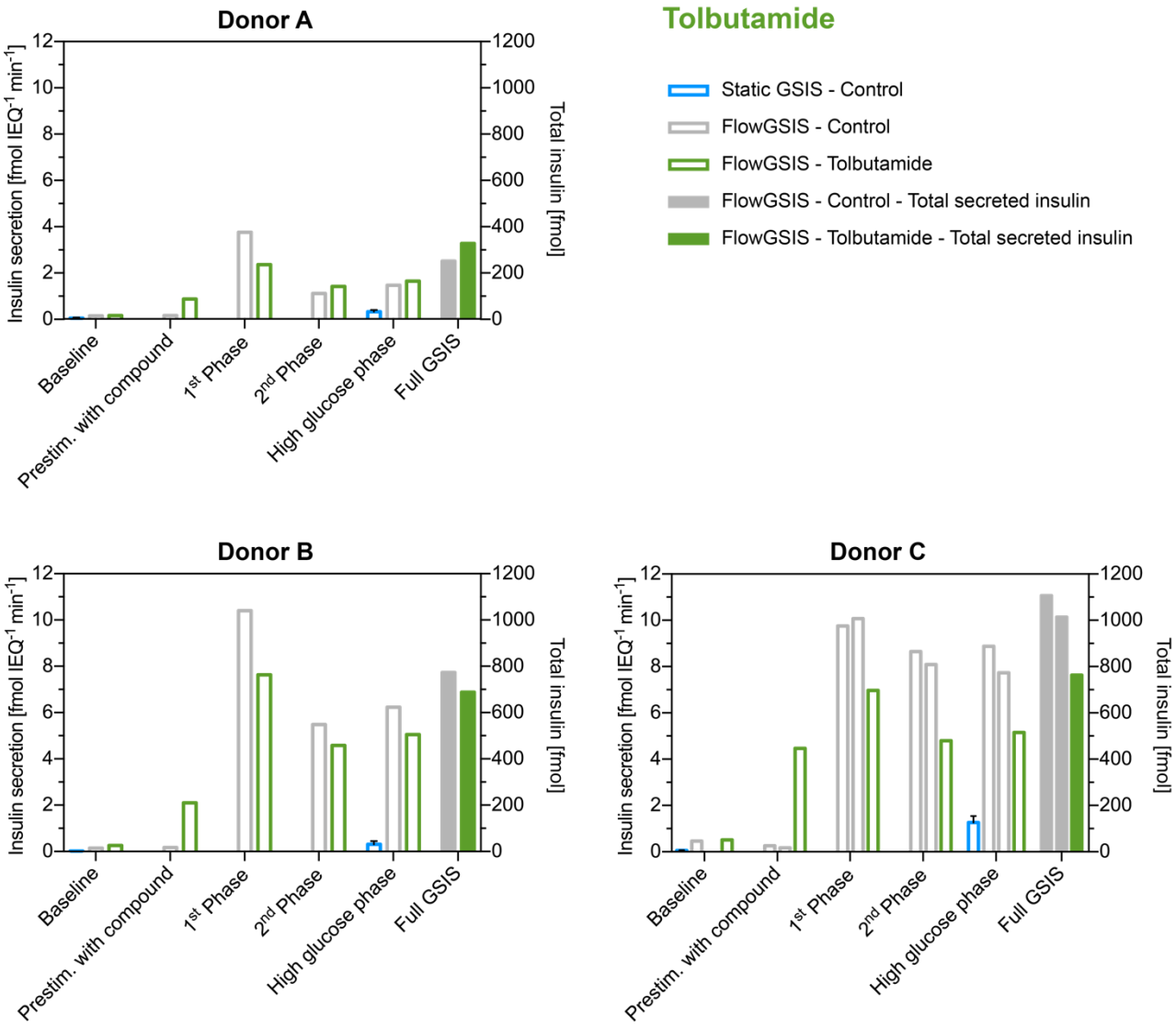

Figure S5: Average insulin secretion rate in each phase of the GSIS (left y-axis), and the total secreted insulin during the full GSIS (right y-axis). Effects of tolbutamide (green) vs. vehicle control (grey) were measured under perfused and static conditions and with islets of three individual donors (A, B and C).

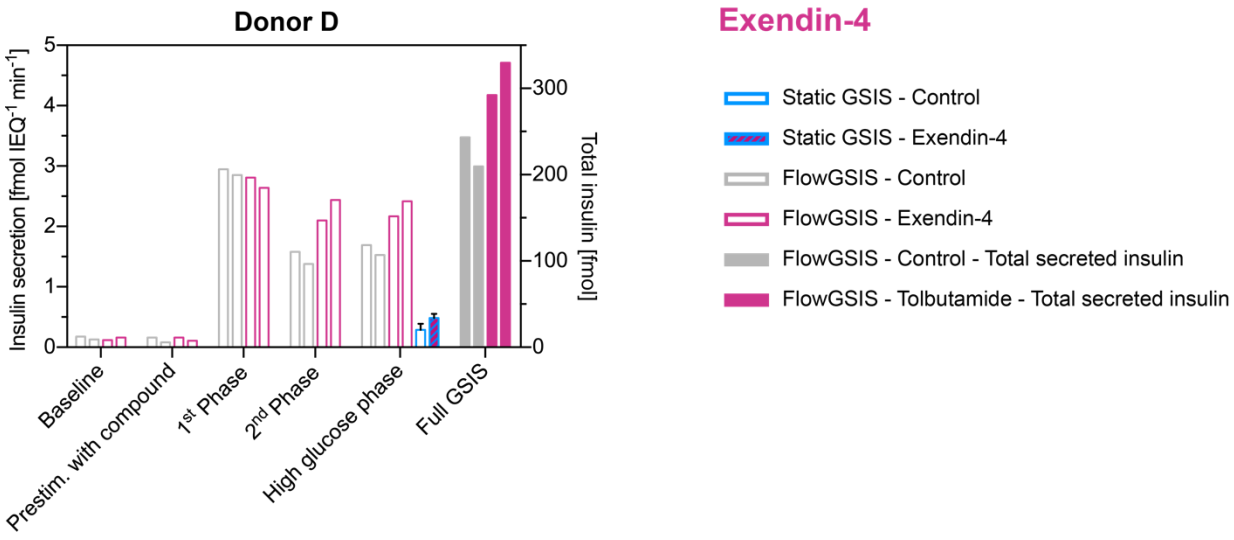

Figure S6: Average insulin secretion rate in each phase of GSIS (left y-axis), and the total secreted insulin during the full GSIS (right y-axis). Effects of 100 nM exendin-4 (purple) vs. vehicle control (grey) were measured under perfused and static conditions with islets of one individual donors (D).

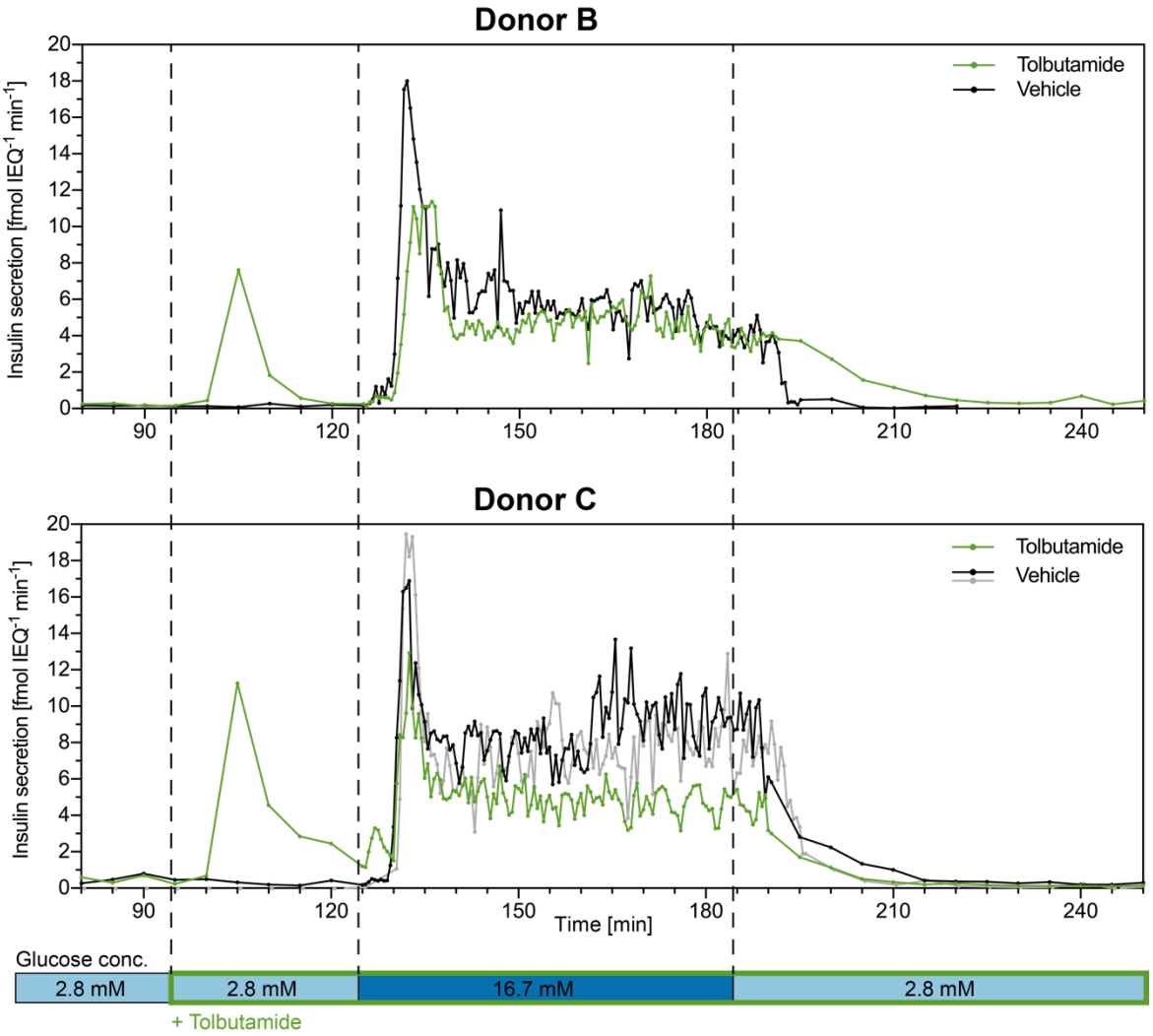

Figure S7: High-resolution FlowGSIS measurements on single islet microtissues from two individual donors (B and C). Islets were treated with 25 µM tolbutamide (green) to assess its effects in comparison to the vehicle control (black and grey). Samples were continuously taken every 5 min during low-glucose conditions (80-125 min and 195-250 min) and every 30 s in the high-glucose phase (125-195 min).

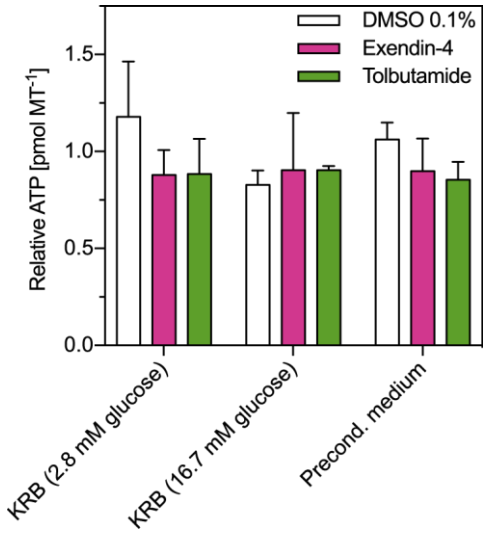

Figure S8: Viability of human islet microtissues. Relative ATP content in human islet microtissues after exposure to compounds in different media. Islets were cultured in a static well plate for 310 min. The ATP content was normalized to that of islets that were cultured in pure medium for each condition (2.8, 16.7 mM glucose (KRB) and preconditioning medium). Three islets were analyzed for each condition (n=3 islets).